



# Interpretation of spring-water temperature variability based on continuous monitoring and numerical modelling of heat transport and water mixing: case study of Czarny Potok spring, Pieniny Mountains, southern Poland

Tomasz Gruszczyński<sup>1</sup> · Marzena Szostakiewicz-Hołownia<sup>1</sup> · Daniel Zaszewski<sup>1</sup>

Received: 21 March 2023 / Accepted: 26 September 2023 / Published online: 19 October 2023  
© The Author(s) 2023, corrected publication 2023

## Abstract

A numerical model of heat conduction and water mixing was developed, enabling a quantitative description of water temperature variability at a spring outflow. The study examined the Czarny Potok spring, located in the Pieniny Mountains of southern Poland, which was the subject of a 4-year series of water temperature observations. The presented model describes the soil and water environment in the immediate vicinity of the spring, assuming that the spring water temperature is shaped by the mixing of water flowing through the shallow zone that experiences seasonal fluctuation and the deeper neutral zone. It was also assumed that the conductive heat flow in the tested medium is conditioned by seasonal heating and cooling of the land surface. The thermal diffusivity of the bedrock was calculated on the basis of the phase shift and the attenuation of thermal amplitude at different depths, based on long-term monitoring of soil temperature. The heat conduction and water mixing models enabled calculation of the water temperature at the outflow. The obtained results are close to the empirical spring water temperatures. The estimated mean error was 0.075 °C and the mean absolute error was 0.188 °C. The results of the calculations suggest that the tested spring is recharged primarily by water flowing through the seasonal fluctuation zone (75%), while the remaining 25% captures a deeper circulation system associated with the neutral zone.

**Keywords** Thermal conditions · Numerical modelling · Heat transfer · Water mixing · Poland

## Introduction

Groundwater temperature is a marker widely used in hydrogeology to trace groundwater circulation (James et al. 2000; Manga 2001; Tamburini and Menichetti 2019; Staško et al. 2021). It is particularly insightful in mountainous and protected areas where the construction and maintenance of complex observation networks is difficult due to terrain conditions and legal restrictions (Birk et al. 2004; Liñán Baena et al. 2009). The observed changes in groundwater

temperature result from a wide spectrum of processes and phenomena occurring in the rock medium—for example, these include changes in the input signal, different heat transfer conditions, water mixing, and differences in flow depth and velocity. However, the interpretation of temperature data in these areas is difficult due to limited information on the structure of the system drained by the springs, the thermal properties of the rock medium, or the spatial and temporal distribution of the heat flux reaching the system.

The interpretation of groundwater temperature data is fundamentally based on the premise that the progressive disappearance of daily, seasonal, and finally annual temperature fluctuations is observed with depth. Correspondingly, the amplitudes of seasonal and annual temperature change decrease with water circulation depth (Taylor and Stefan 2009; Anderson et al. 2013), thus enabling a quick (although qualitative) determination of whether the water drained by the spring is derived from shallow or deep circulation. It is conventionally assumed that changes in shallow

✉ Marzena Szostakiewicz-Hołownia  
marzena.szostakiewicz@uw.edu.pl

Tomasz Gruszczyński  
tgruszcz@uw.edu.pl

Daniel Zaszewski  
danielzaszewski@uw.edu.pl

<sup>1</sup> Faculty of Geology, University of Warsaw, Żwirki I Wigury 93, 02-089 Warsaw, Poland

water temperature are related to changes in air temperature. Cross-correlation analysis and simple linear regression models (Szcucińska and Wasielewski 2013; Doucette and Peterson 2014) are used to describe this relationship and identify the lag in groundwater temperature reaction to air temperature fluctuations. Correlations and models primarily provide information on the existence (or lack thereof) of the relationship between air and water temperatures, and the average lag of groundwater temperature response to changes in air temperature. Linear regression models are also used to predict the average temperature of groundwater in the context of current climate change (Mohseni and Stefan 1999; Figura et al. 2015; Tamburini and Menichetti 2019), but they do not allow for a fully precise description of daily and seasonal groundwater temperature fluctuations. In this shallow zone, water temperatures result from overlapping daily, seasonal, and annual temperature fluctuations. Groundwater temperatures observed at the outflow are additionally influenced by the mixing of different temperature groundwater flowlines.

Broader interpretative possibilities are offered by models describing rock mass heat transport. Even a simple, one-dimensional (1D), black box model, taking into account water mixing, yields novel insights into groundwater circulatory systems (Long and Gilcrease 2009; Gruszczyński and Szostakiewicz-Hołownia 2019). With heat conduction models, the calculation of heat transport in a rock medium, heat-wave-propagation velocity, and heat-wave-amplitude attenuation with depth can be determined. Their application so far mainly relates to the description of heat transport in the unsaturated zone strata medium (Smerdon et al. 2003; Pekárová et al. 2022; Zaszewski and Gruszczyński 2022).

In high-permeability rocks, where groundwater flow is rapid, convection plays the main role in heat transport (Manga 2001). In such a system, numerical models similar to mass transport models are used to describe heat transfer (Munz et al. 2017; Wang et al. 2020; Casillas-Trasvina et al. 2022). The construction of the model and its reliable calibration require a very good recognition of the hydrodynamic conditions and thermal properties of the rock medium, both on the boundaries of the modelled system and within it. For this reason, in mountain catchments, where (1) the availability of input data is low, and (2) the hydrogeological conditions are additionally complicated by tectonic deformation of the rock layers, complex models of heat transport are burdened with high uncertainty and the available dataset is insufficient for their calibration. In such cases, the use of simple mathematical models may be a better solution (Long and Gilcrease 2009).

The following presents the results of work undertaken to quantitatively characterize heat flux in the vicinity of a spring for which a 4-year equal-interval water-temperature-observation series at the outflow was available. In addition, observational sequences of the rock medium temperature

at various depths were generated. A numerical model of heat conduction and water mixing enabled calculation of the water temperature observed in the spring. Apart from describing the quantitative characteristics of the heat transport process, this model also enabled the quantitative separation of the groundwater flowlines supplying the tested spring into (1) a part flowing through the seasonal fluctuation zone and (2) a part representing a deeper circulation system associated with the neutral zone.

## Materials and methods

### Study area

This study examined the Czarny Potok spring, which is located on the southern slopes of the Pieniny Mountains, southern Poland (Fig. 1). The Pieniny Mountains are composed of a portion of the Carpathian chain of mountains. The highest peak of the Pieniny Mountains is Trzy Korony (982 m above sea level) and the lowest point is in the Dunajec Valley (420 m above sea level); as such, the maximum difference in height is 562 m. The climate of the Pieniny Mountains is transitional between Atlantic and continental climates and is mainly influenced by polar-marine air masses (on average, 67% of the year), which drive cooling in summer and warming and thawing in winter. In spring and autumn, there are frequent Arctic air advections (on average, 18.8% of the year) associated with cooling and frost (Dąbrowski and Jaguś 2003). With reference to the classical divisions of Hess (1965), the majority of the Pieniny area (including the investigated source area) belongs to a moderately cool climatic zone, with an average annual air temperature of 4–6 °C and a clear predominance of rainfall over snowfall. The climate of the Pieniny Mountains exhibits characteristic features of mountainous areas, including pronounced spatial diversity. Furthermore, given the latitudinal arrangement of this mountain range, the various slope exposures affect climatic—in particular, thermal—conditions—for instance, on the southern slopes where the investigated spring is located, average annual air temperatures are higher than on the northern slopes (Humnicki 2007). The temperature gradient also varies on each side of the mountain range: on the northern slopes it is 0.26 °C per 100 m, and on the southern slopes, 0.35 °C per 100 m (Kostrakiewicz 1982). Slightly lower rainfall, fewer days with frost, and greater evaporation are observed on the southern slopes as compared to the northern slopes (Humnicki 2007).

Geologically, the study area is part of the Pieniny Klippen Belt, which separates the two main structural units of the Carpathians—the Inner Carpathians and the Outer Carpathians. The geological structure of the Pieniny Klippen Belt is complicated, with the constituent formations strongly

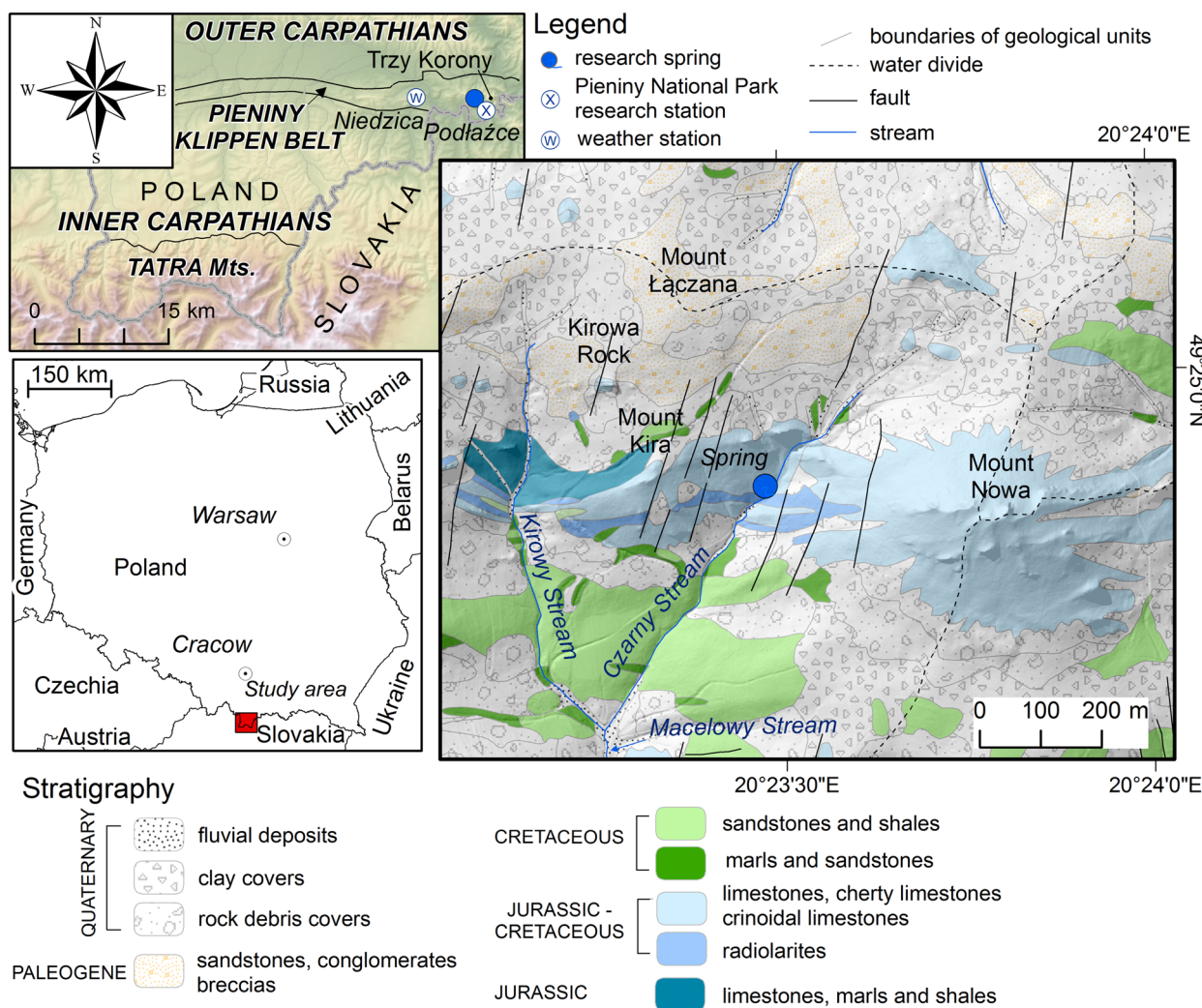


Fig. 1 Location of the Czarny Potok spring over the geological structure background (based on Birkenmajer 2005, 2017)

folded, brecciated, thrust-sheeted, and divided into blocks. Indeed, the Pieniny Klippen Belt is one of the most complex geological structures in Europe (Wierzbowski et al. 2004; Birkenmajer 2017). The high degree of tectonism is associated with the presence of numerous faults, fissures, joints, cleavages, and asymmetric joints. With regards to hydrogeology, the fissures in the Pieniny Mountains play an essential role in groundwater flow through the rock mass and are the dominant conduits supplying spring water; more than 88% of springs in the Pieniny Mountains are considered fissure style (Kibitlewski 1987; Humnicki 2007).

Unsurprisingly, the Czarny Potok spring is a fissure type. The cherty limestones of the Pieniny Limestone Formation are exposed where groundwater flows to the surface, covered to some extent by weathering and rock debris. The spring is located at the south-eastern foot of Mount Kira, 684 m above sea level. It initiates the Czarny Potok, a left-hand tributary of the Macelowy Potok, which in turn flows into the

Dunajec, a regional groundwater drainage base. The entire Czarny Potok Valley is located within Pieniny National Park. In the immediate vicinity of the area examined, there are no anthropogenic heat sources affecting the natural thermal field of the rock mass.

The examined spring is characterized by a constant outflow and a precipitation-melt regime. The summer culmination, associated with rainfall, dominates over the lesser culminations associated with snow cover melting (March) and spring rainfall (May). Based on the average monthly discharges, they should be included in the 6th ( $0.1 - 1 \text{ dm}^3 \text{ s}^{-1}$ ) and, occasionally, in the 5th ( $1 - 10 \text{ dm}^3 \text{ s}^{-1}$ ) Meinzer class. From 2013 to 2017, the highest average monthly discharge of  $1.0 \text{ dm}^3 \text{ s}^{-1}$  was recorded in May and July 2014, and the highest average daily discharge of  $2.4 \text{ dm}^3 \text{ s}^{-1}$  in May 2014. Interpretation of the master recession curves suggests this spring drains one small reservoir with a storage potential of  $2,500 \text{ m}^3$  (Humnicki and Szostakiewicz-Hołownia 2022).

The low discharge of the spring results from the low permeability of the rocks in which the flow takes place within small and tight fissures. The flow is slow and laminar, as confirmed by the absolute isotopic age of the waters exceeding 20 years (Humnicki et al. 2019).

## Field measurements

### Air temperature

Air temperature records were retrieved from the Polish Institute of Meteorology and Water Management Niedzica climate station, which is located ~5.5 km from the examined spring, on the southern slopes of the Pieniny Mountains (Fig. 1). The Niedzica station was built 533.2 m above sea level, below the microclimate zone where the Czarny Potok spring is located; however, there is no record of air temperature for this zone in the analyzed period. The only data from the post near the top of Trzy Korony (982 m above sea level) are incomplete, and do not enable calculations of basic climate indicators (Kozak and Zajac 2018). The main air temperature observation data consist of an average daily air temperature time series; the accuracy of this data was 0.1 °C.

### Soil temperature

Soil temperature values near the observed spring were characterized at the Pieniny National Park meteorological station in Podłaźce (Fig. 1). These measurements were made using five mercury soil thermometers manufactured by Kujawska Wytwórnia Termometrów, which is accredited by the Polish Center for Accreditation (PCA). The thermometers were placed at 5, 10, 25, 50 and 100 cm depths, in line with the recommendations of the World Meteorological Organization regarding the design of environmental monitoring networks (World Meteorological Organization 2018). From 2014–2017, temperature readings were taken by the same observer three times a day at 7:00, 13:00, and 19:00 local time. These values were used to determine the average daily soil temperature at each depth.

### Spring water temperature

A Schlumberger MicroDIVER probe was used to continuously monitor groundwater temperature in the spring. This device records temperature using a built-in semiconductor sensor; the declared measurement accuracy was  $\pm 0.1$  °C, with a precision of 0.01 °C. Field measurements of the spring temperature were taken every 30 min. Measurements performed by the MicroDiver were quarterly controlled with an Eijkelkamp type 18.52.01 device.

The accuracy of the MicroDIVER device was verified using a TERMOPRODUKT Termio-1 thermometer equipped with a platinum PT1000 probe. The accuracy of the reference thermometer was  $\pm 0.05$  °C, with a precision of 0.01 °C. Verification was carried out in a laboratory water bath. The differences between the values measured by the reference thermometer and the MicroDIVER ranged from  $-0.11$  to  $-0.04$  °C—see Fig. S1 in the electronic supplementary material (ESM)—with an average error of  $-0.07$  °C. The errors in the tested temperature range were close to the manufacturer's declared values; nevertheless, the MicroDIVER device was calibrated to minimize measurement errors. The relationship between the MicroDIVER sensor and the reference sensor readings showed a clear linear trend; thus, a linear regression was used to quantify their relationship. The slope for the regressed function was slightly less than 1, resulting in a correction of the MicroDIVER sensor indication by  $-0.037$  °C. This calibration significantly improved the empirical distribution of residual components, which in principle should be close to the normal distribution (Fig. S1 in the ESM). The  $R^2$  coefficient for individual functions is close to 1.

In addition to the description of basic temperature statistics, time series were subjected to additional analyses aimed at identifying the relationship between air and groundwater temperatures, including (1) autocorrelation analysis of time series, enabling the determination of seasonal change frequency; (2) cross-correlation analysis, which enabled the determination of the time shift in the response of the source temperature to the air temperature signal, and (3) linear regression analysis, to determine the fit of both data sets. As in the case of air and soil temperature measurements, the water temperature time series was subjected to discrete Fourier transform (DFT).

## Heat conduction and water mixing model

### Conceptual model

The recharge area of the spring in the Czarny Potok Valley covers a fragment of the active exchange zone, and the water temperature distribution at the outflow depends on heat transport in this zone. The investigated spring is of a descension character, with recharge occurring through underground flow in a cracked rock massif and within the cover formations. The water temperature at the outflow is determined by heat transport in the seasonal temperature fluctuation zone and the neutral zone. The spring drains the fissure medium in which a slow laminar flow takes place. Based on the research results of Manga (2001) and Luhmann et al. (2011), it was assumed that heat transport occurs mainly as a result of conduction in zones of seasonal fluctuations. The temperature of the water–rock system approaches, with

depth, the value typical for the neutral zone, which is usually close to the average annual air temperature (Williams and Gold 1976). Due to the shallow water table in the vicinity of the source, the heat flux occurs primarily in the saturation zone and two mutually perpendicular heat flows must be considered. The first is related to heat conduction due to net incoming radiation. For this flux, the vertical advective component is negligible due to the limited thickness of the aeration zone and the dominant horizontal component of water movement in the saturation zone. The second heat flux is related to groundwater flow advection, and can be divided into two parts (Fig. 2).

The former (a, Fig. 2) includes a fragment of the groundwater flowline flowing through both the neutral zone and the seasonal fluctuation zone. At the contact between these zones, the horizontal temperature gradient will be nonzero, and its value (and thus the intensity of the heat advection flux) will decrease along with the groundwater flow towards the spring. The latter part of the groundwater flowline (b, Fig. 2) only covers the neutral zone, in which the temperature gradient, and thus the intensity of the advective heat flux, is negligibly small.

### Mathematical model

The aforementioned considerations were the basis for a mathematical model of heat transport, enabling one to calculate groundwater temperature flowing to the surface. Due to the impossibility of recognizing, in detail, the

actual temperature gradients in the rock mass, the following assumptions are necessarily simplifications.

1. The outflow water temperature is a combination of the temperature of water flowing in the seasonal fluctuation zone and the neutral zone:

$$T_z = \alpha \bar{T}_a + (1 - \alpha)T_b \tag{1}$$

where  $T_z$  (°C) is the spring water temperature,  $\bar{T}_a$  (°C) is the mean water temperature in the seasonal fluctuation zone,  $T_b$  (°C) is the water temperature in the neutral zone, and  $\alpha$  is the portion of water inflow to the source from seasonal fluctuation zones.

2. The water temperature in the neutral zone is constant, and close to the average annual air temperature (Williams and Gold 1976).
3. Water temperature in the seasonal fluctuation zone is variable in time and space. In the immediate vicinity of the spring, this variability is a consequence of heat conduction directed perpendicular to the ground surface. The advection term can be neglected due to small horizontal temperature gradients in the vicinity of the spring.
4. The heat flux along the normal to the ground surface varies in time, resulting directly from the variability of the net incoming radiation.
5. Heat conduction occurs in a homogeneous medium due to thermal diffusivity.
6. In combination, assumptions 4 and 5 enable the use of the 1D heat conduction equation to describe heat transport in the seasonal fluctuation zone (Taylor and Stefan 2009):

$$\lambda \frac{\partial^2 T}{\partial z^2} = c_p \rho \frac{\partial T}{\partial t} \tag{2}$$

where  $T$  is temperature of the medium (°C),  $\lambda$  is coefficient of thermal conductivity of the medium ( $\text{W m}^{-1} \text{K}^{-1}$ ),  $c_p$  is specific heat of the medium ( $\text{J kg}^{-1} \text{K}^{-1}$ ),  $\rho$  is density ( $\text{kg m}^{-3}$ ),  $z$ ,  $t$  are variables of space and time, respectively.

Equation (2) can be solved numerically using the finite difference method (Pletcher 2006). Implicitly, the differential analog of this equation for a homogeneous medium can be written as:

$$\lambda \frac{T_{i-1,j+1} - 2T_{i,j+1} + T_{i+1,j+1}}{\Delta z^2} = c_p \rho \frac{T_{i,j+1} - T_{i,j}}{\Delta t} \tag{3}$$

where  $i$ ,  $j$  are indices describing points in space and time, respectively; and  $\Delta z$  and  $\Delta t$  are space and time discretization steps, respectively. An implicit scheme was used to derive the difference analog. Equation (3) should be written

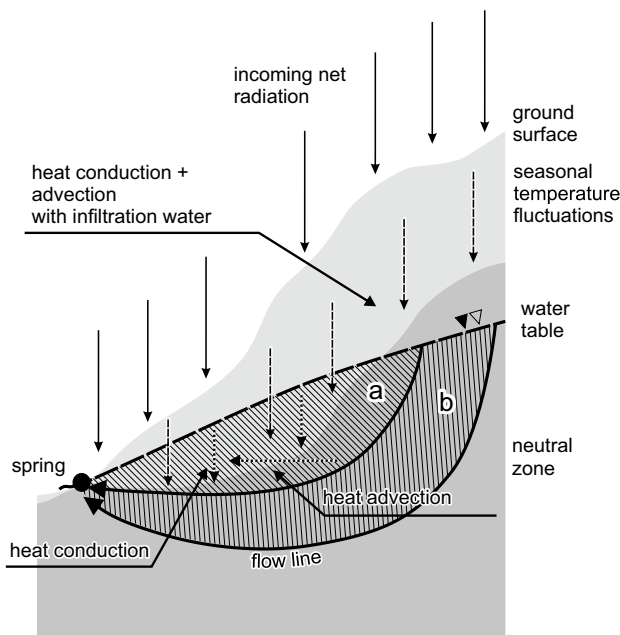


Fig. 2 Conceptual model of heat transport in the discharge area of the Czarny Potok spring

independently for each discrete space–time point, but it is more convenient to use its equivalent form:

$$T_{i-1} + UT_i + T_{i+1} = -WT_i^*, \quad W = \frac{\Delta z^2}{D\Delta t}, \quad U = -2 - W \quad (4)$$

where  $D = \frac{\lambda}{c_p \rho}$  is the thermal diffusivity of the medium,  $U$  and  $W$  are parameters depending on thermal diffusivity and discretization of time and space,  $T$  is the temperature in the current time step, and  $T^*$  is the temperature in the preceding step (i.e., the initial condition). With this procedure, a system of linear equations in each time step can be formulated and written in matrix form:

$$\mathbf{A} \cdot \mathbf{h} = \mathbf{rhs} \quad (5)$$

where  $\mathbf{A}$  is the coefficient matrix,  $\mathbf{h}$  is the unknowns vector, and  $\mathbf{rhs}$  is the right hand vector. The following boundary and initial conditions were adopted to solve the aforementioned system:

$$T(z = 0, t) = f(t), \quad T(z = L, t) = T_p = \text{const}, \quad T(z, t = 0) = f(z) \quad (6)$$

where  $L$  is the thickness of the seasonal fluctuation zone, and  $T_p$  is the multiyear average annual air temperature. After the boundary and initial conditions have been formulated, the system of linear equations can be solved sequentially using any iterative algorithm. It is worth noting that the coefficient matrix is sparse, and its nonzero elements cluster only on three diagonals. Eventually, with constant  $\Delta t$ , this matrix is invariant for each time step. To determine  $\mathbf{A}^{-1}$  an existing SOLVER included with the Python NumPy package and the technique of matrix LU decomposition with partial pivoting was used (Okunev and Johnson 1997). As such, a high numerical efficiency algorithm was developed, which broadly consisted of determining the approximate matrix inverse to  $\mathbf{A}$ . As such, the iterative solution of Eq. (5) in each time step was abandoned, and the unknowns vector could be found directly using the equation:

$$\mathbf{h} = \mathbf{rhs} \cdot \mathbf{A}^{-1} \quad (7)$$

After solving the system of equations in all time steps, the model returns a two-dimensional (2D) array representing the spatiotemporal temperature distribution in the seasonal fluctuation zone in the immediate vicinity of the spring. To determine the outflow water temperature, it is necessary to use a water mixing model that includes water flowing into the spring from both zone (a) and the neutral zone (b). Assuming that the groundwater flowlines are uniform, the temperature in zone (a) can be determined by the average value of the vector  $\mathbf{h}$  in each time step (Fig. 4). It should be noted that in the case of the analysed medium,

this assumption does not have to be fully met. Groundwater flow takes place in this case in a fissured medium, and the filtration paths form a complex system. In addition, the width of the fissures strongly depends on the degree of rock mass relaxation and decreases with depth. Due to the limited measurement availability of the system, it is impossible to identify changes in the water permeability of the medium with depth (the study area is located in a protected zone). Therefore, and due to the fact that the calculations apply only to the near-surface zone (up to a depth of 6 m), the authors decided to treat the groundwater flow field as homogeneous. Then, the outflow water temperature can be calculated via Eq. (1). The proportional share of these sources in the spring recharge is determined by the  $\alpha$  parameter, the value of which is determined by successive approximations during model calibration.

One-dimensional heat flux calculations were made using the finite difference method. The calculation space was divided into 20 blocks using (at first) a constant spatial discretization step  $\Delta z = 0.5$  m, and time discretization with a constant step  $\Delta t = 1$  day. The space was treated as homogeneous due to its ability to conduct and store heat. For the calculations, a constant value of thermal diffusivity of  $0.043 \text{ m}^2 \text{ day}^{-1}$  was adopted, as obtained based on the phase shift of soil temperature curves. Relations with the external environment are described using Dirichlet boundary conditions. The boundary corresponding to the land surface was assigned a time-varying value, based on soil temperatures measured at 5 cm depth. On the opposite boundary, corresponding to the upper border of the neutral zone, a constant temperature of  $6 \text{ }^\circ\text{C}$  was set, which is a value close to the average annual air temperature in the ridges of the Pieniny Mountains. The calculation procedure consisted of two stages. First,  $\bar{T}_a$  ( $^\circ\text{C}$ ) was determined by averaging the temperature values obtained from the model in the entire seasonal fluctuation zone for each time step. For this purpose, the arithmetic average of temperatures obtained in individual computational blocks was calculated, which was justified due to the constant space discretization step in the model and the assumption of groundwater flowline homogeneity. The next step consisted in selecting the  $\alpha$  parameter, which determines the proportion of flowline representing individual zones supplying the examined spring. As a result, it was possible to calculate spring temperature at the outflow, and the calculation result could be compared directly with empirical data. This provided the basis for the model calibration procedure. During calibration, the coefficient  $\alpha$  and the neutral zone temperature were selected. The unknown depth of the neutral zone was also examined by varying the space discretization step  $\Delta z$ .

## Results

### Air temperature results

The average air temperature in 2014–2017 was 7.66 °C, with a standard deviation of 7.82 °C (Table 1). Average annual air temperatures steadily decreased from 8.15 °C in 2014 to 7.11 °C in 2017. Strong short-term fluctuations are observed in the temporal temperature distribution (Fig. 3). The variability is particularly clear in winter, when differences in average daily temperatures can reach up to ~20 °C in less than 1 week. Winter air temperatures were largely the drivers of average annual values; winters in 2016 and 2017 were colder than in 2014 and 2015, and low temperatures also lasted longer in the later years, translating into low average annual values despite relatively warm summer periods. The influence of winter on shaping average annual air temperatures is also clearly visible in 2014, which has the highest annual

**Table 1** Variation of annual air temperature (°C) values, expressed by means of basic statistics. *SD* standard deviation

Year	Minimum	Maximum	Average	SD
2014	-13.8	20.2	8.15	6.95
2015	-15.7	24.1	7.96	7.87
2016	-14.4	22.8	7.43	7.99
2017	-20.1	23.4	7.11	8.38
2014–2017	-20.1	24.1	7.66	7.82

average in the analyzed period despite the relatively cool summer. The annual air temperature distribution was characterized by four clearly distinct seasons, typical for temperate climates—the summer period, with average monthly temperatures above 15 °C, occurred in June–August; the winter period, with average monthly air temperatures below or close to 0 °C, was in December–February.

The seasonal change signal was separated using DFT, as determined on the basis of the dominant spectral power. The seasonal change frequency was 0.0027 day<sup>-1</sup>, which translates into a period of 365 days (Fig. 4). The air temperature-change amplitude reached 9.87 °C.

### Soil temperature results

Soil data provided information on the rock medium temperature variability from the surface to 1 m below ground level. These data were arranged as equal interval time series, which consisted of average daily temperature values at individual depths in 2014–2017. In each analyzed series, the recorded temperature variability was seasonal, and closely related to typical mid-latitude net solar radiation. Above 25 cm depth, high-frequency signals and ‘white noise’ signals are clearly visible in the temperature variability (Fig. 5). These signals are low amplitude, and similar to the short-term air temperature variability. The average temperatures at individual depths are similar, ranging from 10.06 to 10.87 °C (Table 2). These values are higher than the average annual air temperature at the Niedzica station (7.66 °C).

**Fig. 3** Concept of the heat conduction and water mixing model near Czarny Potok spring

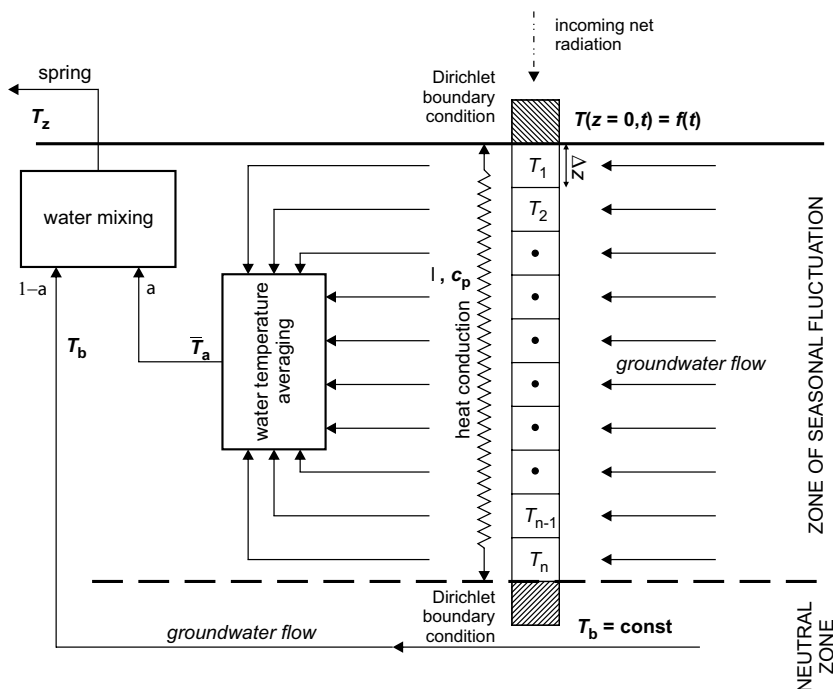


**Fig. 4** Plot of periodic functions for seasonal changes in air temperature (red line) and spring water temperature (blue line) over the background of average daily air temperatures at the Niedzica station and groundwater waters drained by the Czarny Potok spring in years 2014–2017

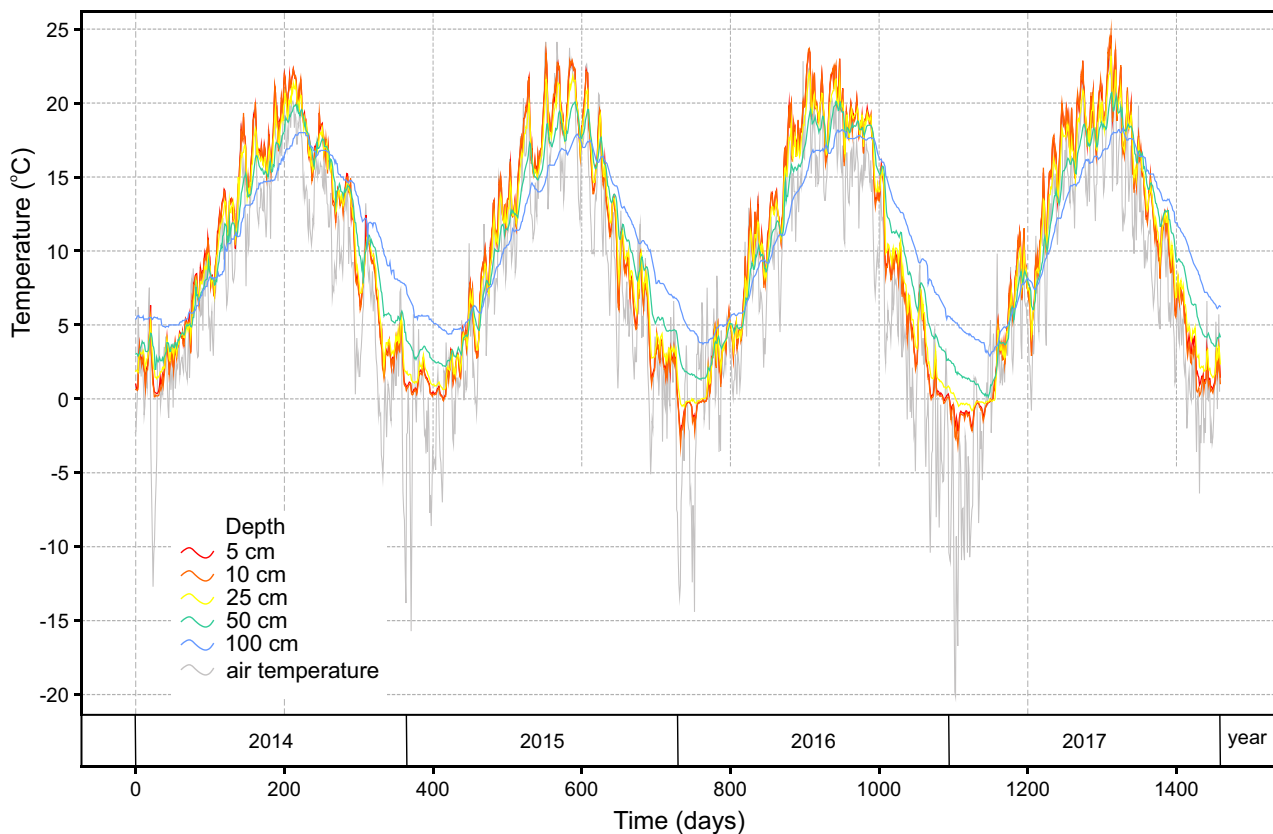
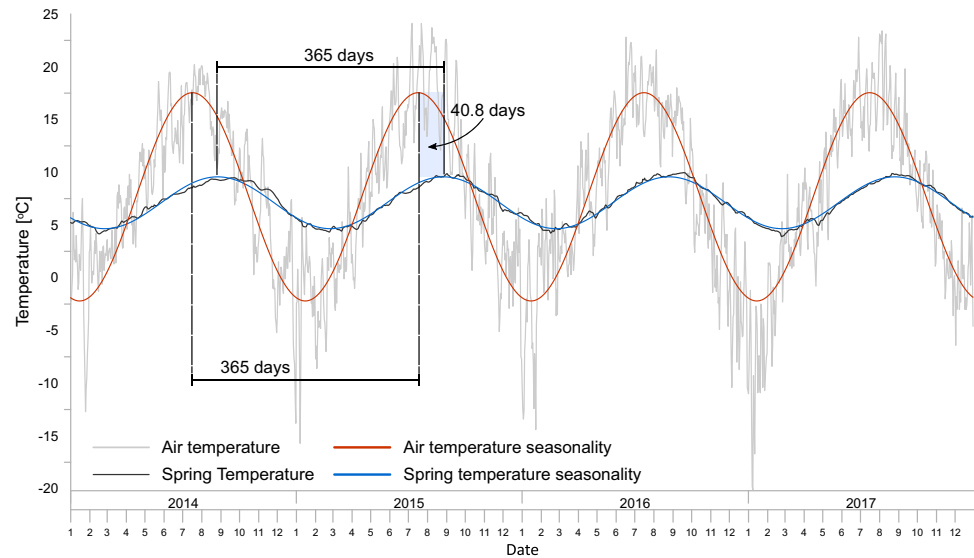


**Fig. 5** Temperature variability of the soil medium at different depths in the years 2014–2017 and average daily air temperatures at the Niedzica station

The annual heat wave amplitude clearly attenuates with depth, as confirmed by the standard deviation values for individual soil temperature time series. At 5 cm depth, the standard deviation is 7.37 °C; the standard deviation

sequentially decreases to 4.66 °C at 100 cm depth (Table 2). Individual time series were analyzed using DFT to quantitatively characterize wave attenuation, clearly distinguishing the dominant signal, corresponding to a frequency of



**Table 2** Time series statistics representing the variability of the temperature of the rock medium at different depths in the years 2014–2017. *SD* standard deviation

Depth (cm)	Temperature descriptive statistics		DFT results	
	Average (°C)	SD (°C)	Amplitude (°C)	Phase shift (days) relative to air temperature curve
5	10.06	7.37	10.07	3.0
10	10.17	7.30	9.99	3.4
25	10.14	6.83	9.40	6.5
50	10.36	5.95	8.25	15.5
100	10.87	4.66	6.45	27.7

**Table 3** Water temperature variability (°C) at the outflow from the Czarny Potok spring, expressed by basic descriptive statistics. *SD* standard deviation

Year	Minimum	Maximum	Average	SD
2014	4.16	9.48	7.17	1.71
2015	4.32	9.86	7.01	1.81
2016	4.23	9.96	7.21	1.82
2017	3.90	9.88	7.03	1.86
2014–2017	3.90	9.96	7.11	1.80

0.00274 day<sup>-1</sup> (period 365 days), from higher frequency signals and white noise. Using this procedure, both the amplitude and the phase shift of the heat wave at each depth could be determined (Table 2), demonstrating that the heat wave amplitude attenuated with depth, from 10.07 °C at 5 cm depth to 6.45 °C at 100 cm depth; the phase shift between these depths is up to 25 days. Both the wave amplitude attenuation and increasing phase shift with depth are typical of heat wave propagation due to heat conduction in the rock medium. Both phenomena result from the thermal diffusivity of the medium. According to the wave propagation model, the thermal diffusivity can be estimated independently for both phenomena. Thus, for this purpose, an analytical model of heat conduction in a semi-infinite system was used, whereas for the analyzed spring, both the attenuation and phase shift suggest the thermal diffusivity was ~0.04 m<sup>2</sup> day<sup>-1</sup>.

### Spring water temperature results

In the analyzed period, the average annual spring water temperature at the outflow was 7.11 °C, with a standard deviation of 1.80 °C. The average annual temperature was similar in each year, with a maximum difference of 0.2 °C. The highest average daily water temperatures (9.96 °C) were recorded on 18–19 September 2016, and the lowest (3.90 °C) on 24 February 2017 (Table 3). Cyclical changes in spring water temperature were observed throughout the research period (Fig. 4). In a given annual cycle, the

maximum daily values were observed in August–September, while the minimum occurred in February. The seasonality of groundwater temperature changes is confirmed by the auto-correlation coefficient. The length of a single change cycle is exactly 365 days, the same seasonality observed for air temperatures (Fig. 6a).

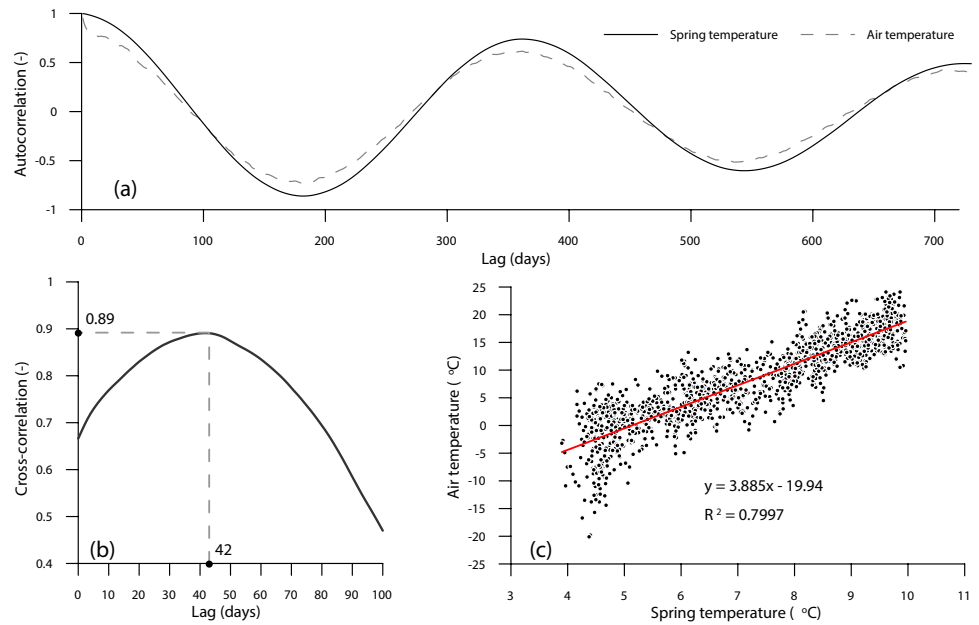
A correlation between air and spring water temperatures was also observed, with a clear lag in the temperature response of waters and a shift of extreme values to late winter and late summer (Fig. 4). These observations are confirmed by both linear regression analysis and cross-correlation analysis between air and spring water temperatures (Fig. 6b, c). In cross-correlation analysis, the correlation value depends on the phase shift of the temperature curves. The maximum correlation value (0.89) occurs with a phase shift of 42 days, demonstrating the strong connection between air and groundwater temperatures (Fig. 6b). The coefficient of determination ( $R^2$ ), characterizing the goodness of fit accounting for the 42-day delay in groundwater temperature response, was 0.7997, suggesting a very strong fit.

Analyzing the air, soil and spring water temperature time series via DFT returned identical seasonal change periods of 365 days (Fig. 4). The periodic function amplitude of water temperature was 2.46 °C, 7.5 °C lower than the seasonal oscillation amplitude of air temperature and 4 °C lower than the ground temperature amplitude at 100 cm depth. The short-term signals observed in air and shallow soil temperatures are not visible in the spring water temperature measurements. There is a distinct phase shift between the extreme values of the periodic functions of air and spring water temperatures. They differ by 40.8 days, which is very close to the 42 days suggested by cross-correlation.

### Model results

The best fit of model results to the empirical data was obtained for  $\alpha=0.75$ , a neutral zone temperature of 5.5 °C, and  $\Delta z=0.3$  m. The fit of calculation results to the empirical data is shown in Fig. 8b. The mean error (ME=0.075 °C) and the mean absolute error (MAE=0.188 °C) were

**Fig. 6** Autocorrelation function, **b** cross-correlation function, and **c** linear regression model determined for the Czarny Potok source in 2014–2017



calculated to quantify the goodness of fit based on the residuals. These low error values indicate that the developed model, despite the adopted simplifications, explains the observed variability of water temperature reasonably well.

The heat conduction results in the near-surface zone are shown in Fig. 7a, enabling one to trace temperature variability across the entire depth profile of the seasonal fluctuation

zone. The calculations indicate a strong connection between the temperature of the near-surface zone medium and the temperature of the active surface. In the shallowest zone, there is short-term variability, and clear temperature changes can even be observed daily. With increasing depth, the temperature amplitude attenuates due to heat transport, and short-term changes become more difficult to distinguish.

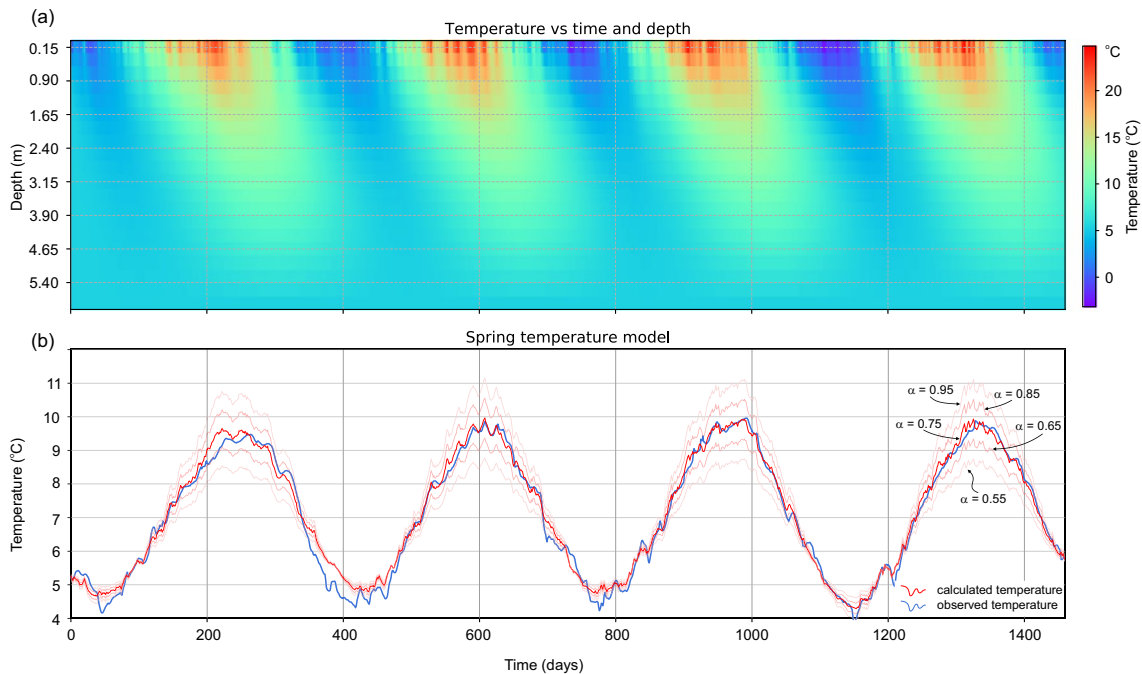


**Fig. 7** **a** The calculated temperature distribution of the soil medium in the zone of seasonal fluctuations and **b** the fitting of the measured and calculated spring water temperatures

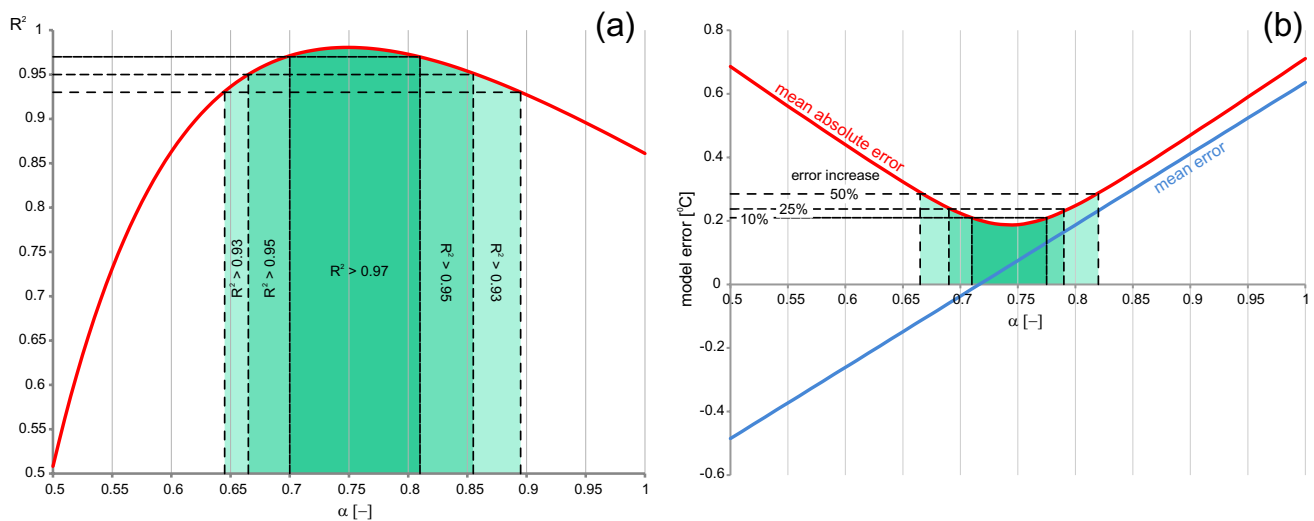


**Fig. 8** Assessment of the sensitivity of the model to changes in the  $\alpha$  parameter **a** using  $R^2$  and **b** mean absolute error as an argument of object function

In addition, the thermal diffusivity of the medium causes a clear temporal shift of individual peaks. This phenomenon is exhibited by the previously mentioned lag in the spring's response to air temperature changes.

The simple water mixing model adopted in the calculations made it possible to estimate the share of the groundwater flowline associated with the seasonal fluctuation zone ( $\alpha=0.75$ ) and the flowline representing the inflow from the neutral zone ( $1 - \alpha=0.25$ ). The results indicate that the spring mainly drains water from the near-surface zone; however, a significant amount of the inflow is associated with the vertical component, representing a deeper circulation system associated with the neutral zone.

The calculated value of parameter  $\alpha$  indicates the share of water that comes from the zone of seasonal fluctuations in the recharge of the investigated spring. This value should be treated as a key result of the calculations; thus, for this reason it was decided to perform a sensitivity analysis for the model. Changes in the value of parameter  $\alpha$  significantly translate into the degree of model fit, especially in the periods when the largest amount of thermal energy is stored in the medium (Fig. 7b). With an increase of the value of parameter  $\alpha$ , the amplitude of the water temperature curves returned by the model decreases. This translates directly into the model fit metrics (Fig. 8). The  $R^2$  coefficient reaches its maximum (0.9806) for parameter  $\alpha$  at the level of 0.75. Deflection from this value causes the  $R^2$  to decrease, but these changes occur faster during decrease of parameter  $\alpha$ . It should be noted that at values of parameter  $\alpha$  between 0.7 and 0.81,  $R^2$  remains very high (above 0.97), which indicates fit uncertainty. A similar uncertainty range was also obtained in the analysis of MAE changes. In this case, choosing the value of parameter  $\alpha$  beyond the range of 0.69–0.79 resulted

in an increase in the MAE value exceeding 25% of the error obtained for the best fit. Concluding, it was assumed that, taking into account the uncertainty of the calculations, the obtained value of the share of shallow waters in the spring recharge can be estimated as  $\alpha=0.75 \pm 0.05$ .

## Discussion

Given the absence of a recognized structure for the spring water system, a black box heat transfer and water mixing model was developed to identify the processes shaping the spring's temperature. In this system, the output was the water temperature of the Czarny Potok spring. The model assumed that its value resulted from the mixing of groundwater flowing through the seasonal fluctuation zone and the neutral zone. The input was a time-varying heat flux transferred to the deeper parts of the bedrock.

An important issue during model development was to appropriately characterize the heat flux reaching the system. As outlined previously, an analysis of air temperature (for the Niedzica meteorological station) and spring water temperature showed a relationship between both series. Specifically, in the case of the Czarny Potok spring, the most significant correlation ( $R=0.89$ ) occurred when the lag in the reaction of the spring temperature to changes in air temperature (42 days) was considered. Identical seasonal periodicity (365 days) was recognized after comparing the DFT results for both series. The difference in phase shifts was 40.8 days, close to the results obtained from correlation methods; however, suggesting that air temperature was the main factor influencing groundwater temperature may be misleading. The air temperature measurements presented here refer to

a meteorological station located close to a large valley and water reservoir, about 150 m lower than the spring outflow elevation. The microclimate conditions and the air flow are therefore different than in a deeply cut, narrow valley higher in the mountain sequence. Moreover, the location itself is not the only factor limiting the usefulness of air temperature data in this model. Air temperature is only one of many elements shaping ground temperature, which also depends on the net incoming solar radiation flux, soil absorption capacity (depending on the type of active surface), active surface exposure, cloudiness, precipitation, snow cover, and evaporation (van Wijk 1965; Williams and Gold 1976; Fleagle and Businger 1980; Zhang 2005; Wojkowski and Skowera 2017; Dafflon et al. 2022). The significant correlation between the air and groundwater temperatures might be driven by the fact that both variables are substantively affected by solar radiation (Allan and Castillo 2007; Kurylyk et al. 2015); therefore, resulting from the influence of the preceding factors, it was decided to adopt soil temperature, measured at 5 cm depth, as the upper boundary of the model. Surreptitiously, this solution also eliminated the need to calculate the ground heat flux using an additional dataset or simplifying assumptions, making this approach to source temperature modeling more universal, at least in areas with limited observational data. However, air temperature data provide good background for considering seasonal influences on the spring water temperature.

The model considers only conductive heat transfer, and assumes that this zone is homogenous in terms of thermal diffusivity. DFTs showed that the ground and source temperature time series are characterized by an identical period (365 days), a progressively increasing phase shift and a rapid attenuation of short-term temperature changes. These features are typical of heat wave propagation because of conduction in the rock medium. Quantification of the phase shift and amplitude attenuation enabled estimation of the thermal diffusivity for the shallow bedrock ( $0.043 \text{ m}^2 \text{ day}^{-1}$ ). This value is consistent with those recorded from formations with a significant silty fraction (Thomson 2010; Arkhangelskaya 2020), including weathering deposits, and also aligns with those from carbonate weathering debris (Polyakov et al. 2021). It should be noted, however, that the obtained thermal diffusivity applies to an unsaturated medium, and is not representative of the saturation zone in the vicinity of the tested spring. Therefore, the actual thermal diffusivity of the tested medium remains unknown, and cannot be determined by calibration of the model—a classic inverse problem. To elaborate, in the presented model (Eq. 4), the control parameter in the heat conduction calculation process is  $W$ , the value of which depends on both the diffusivity and the space discretization step ( $\Delta z$ ). Since  $\Delta z$  directly depends on the unknown and a priori assumed thickness of the seasonal fluctuation zone, it naturally follows that there are infinitely many sets

of  $D$  and  $\Delta z$  for which the model will return the same result. Despite the use of a deterministic heat conduction model, the developed model is a classic black box due to this method's inability to recognize the state function inside the system. This model enables the correct calculation of water temperature at the outflow, but the parameter suite used for this purpose (thermal diffusivity and seasonal fluctuation zone thickness) is subject to uncertainty and cannot be directly interpreted. Here, the constant diffusivity value was previously established for the unsaturated zone; thus, treating this quantity as immutable,  $W$  was determined by selecting  $\Delta z$ . The best fit was obtained with  $\Delta z = 0.3 \text{ m}$ . In the spatial discretization scheme, this means that the seasonal fluctuation zone thickness in the vicinity of the spring is 6 m, which is relatively thin. In a temperate climate, the neutral zone depth (depending on the rock medium) may reach 15–20 m (Williams and Gold 1976; Rybach 2012). Nevertheless, in the groundwater drainage zones, the advection stream directed towards the ground hinders the propagation of the surficial temperature signal, thereby attenuating it faster (Kurylyk et al. 2015). In view of the foregoing considerations, it is not possible to determine accurate and reliable thermal diffusivity and neutral zone depth values in the presented heat transfer model. That being stated, it is also not necessary for the model to function, because its accuracy is determined by the final value of  $W$ , not by individual components.

Despite the simplifications used in the model, a good fit of the calculated output (spring water temperature) to the measurement data was obtained, as evidenced by the low mean error ( $0.075 \text{ }^\circ\text{C}$ ) and mean absolute error ( $0.188 \text{ }^\circ\text{C}$ ). This suggests that the model correctly describes and explains water temperature variability at the Czarny Potok spring outflow. Indeed, the modeling results confirm that the tested spring drains water flowing through the seasonal fluctuation zone. However, this alone does not determine the model's value, as this conclusion can be formulated using classical correlation and DFT methods alone. An important advantage here, however, is the quantitative description of the proportion of waters coming from both the (1) seasonal fluctuation zone and (2) neutral zone. Here, it was determined that 75% of water in Czarny Potok spring comes from the seasonal fluctuation zone, while 25% comes from the neutral zone. Moreover, the presented model enables calculation of the temperature of water flowing through the neutral zone. The best agreement between calculations and empirical data suggests the water temperature in the neutral zone was  $5.5 \text{ }^\circ\text{C}$ . The water flowing through this zone represents the deeper parts of the source supply system. The water temperature of the neutral zone is constant, and should be close to the average annual air temperature (Williams and Gold 1976). Indeed, the obtained temperature is close to the average annual air temperature in the ridges of the Pieniny

Mountains (5.3–6.4 °C; Kozak and Zajac 2018). It can therefore be assumed that the main areas of groundwater recharge, related to circulation within the neutral zone, are the high outcrops that build the Pieniny mountain ranges.

## Conclusions

The heat flow model described in this article allows for a quantitative characterization of temperature variability across the seasonal fluctuation zone. However, this model can only be calibrated based on spring temperature data. In this approach, the heat transfer model was treated as a component of a more complex model, taking into account the mixing of waters from the seasonal fluctuation zone and the neutral zone.

Despite simplifications, a high degree of agreement between the empirical data and the model results was obtained, as evidenced by the low error values (ME = 0.075 °C, MAE = 0.188 °C). Low error values also suggest that the developed model reasonably explains the water temperature variability observed at the spring outflow.

Due to this water mixing model, it is possible to quantitatively determine the proportion of waters from the seasonal fluctuation zone and the neutral zone. The results of the calculations show that the examined spring mainly drains water from the shallow circulation zone (75%), the temperature of which is conditioned by heat conduction in the near surface environs. However, an important part of the inflow is the water stream from the neutral zone (25%); thus, measurements of shallow ground layer temperatures can be used to characterize the heat flux transferred to the deeper parts of the bedrock.

**Supplementary Information** The online version contains supplementary material available at <https://doi.org/10.1007/s10040-023-02729-z>.

**Acknowledgements** The authors would like to thank the management and employees of Pieniny National Park for their kindness and for providing access to meteorological data and the results of soil temperature measurements.

**Funding** The development of the mathematical model and software was supported by project funding *Multidimensional analysis of the changes in the natural thermal field of the soil medium resulting from artificial heat source effects (BOB-661-131/2022) obtained in the programme Green University of Warsaw (as part of the internal grant system at the University of Warsaw). The fieldwork was carried out under the National Science Center (Poland) grant No. 2011/03/D/ST10/05382.*

## Declarations

**Conflict of interest** On behalf of all authors, the corresponding author states that there is no conflict of interest.

**Open Access** This article is licensed under a Creative Commons Attribution 4.0 International License, which permits use, sharing, adaptation, distribution and reproduction in any medium or format, as long as you give appropriate credit to the original author(s) and the source, provide a link to the Creative Commons licence, and indicate if changes were made. The images or other third party material in this article are included in the article's Creative Commons licence, unless indicated otherwise in a credit line to the material. If material is not included in the article's Creative Commons licence and your intended use is not permitted by statutory regulation or exceeds the permitted use, you will need to obtain permission directly from the copyright holder. To view a copy of this licence, visit <http://creativecommons.org/licenses/by/4.0/>.

## References

- Allan JD, Castillo MM (2007) Stream ecology: structure and function of running waters, 2nd edn. Springer, Dordrecht, The Netherlands
- Anderson RS, Anderson SP, Tucker GE (2013) Rock damage and regolith transport by frost: an example of climate modulation of the geomorphology of the critical zone. *Earth Surf Process Landforms* 38:299–316. <https://doi.org/10.1002/esp.3330>
- Arkhangelskaya TA (2020) Parameters of the thermal diffusivity vs. water content function for mineral soils of different textural classes. *Eurasian Soil Sci* 53:39–49. <https://doi.org/10.1134/S1064229320010032>
- Birk S, Liedl R, Sauter M (2004) Identification of localised recharge and conduit flow by combined analysis of hydraulic and physico-chemical spring responses (Urenbrunnen, SW-Germany). *J Hydrol* 286:179–193. <https://doi.org/10.1016/j.jhydrol.2003.09.007>
- Birkenmajer K (2005) Pieniński Park Narodowy, Mapa geologiczna w skali 1:5000 [Pieniny National Park, geological map, scale 1: 5 000]. Pieniński Park Narodowy, Krościenko nad Dunajcem, Poland
- Birkenmajer K (2017) Geologia Pienin [Geology of the Pieniny Mountains, West Carpathians, Poland]. Pieniński Park Narodowy, Krościenko nad Dunajcem, Poland
- Casillas-Trasvina A, Rogiers B, Beerten K, et al (2022) Characterizing groundwater heat transport in a complex lowland aquifer using paleo-temperature reconstruction, satellite data, temperature-depth profiles, and numerical models. *Hydrol Earth Syst Sci* 26:5577–5604. <https://doi.org/10.5194/hess-26-5577-2022>
- Dąbrowski D, Jaguś A (2003) Występowanie układów barycznych, mas powietrza i frontów atmosferycznych nad regionem pienińskim [Occurrence of pressure systems, air masses and atmospheric fronts over the Pieniny Mts. region]. *Pieniny - Przyr i Człowiek* 8:53–61
- Dafflon B, Wielandt S, Lamb J et al (2022) A distributed temperature profiling system for vertically and laterally dense acquisition of soil and snow temperature. *Cryosph* 16:719–736. <https://doi.org/10.5194/tc-16-719-2022>
- Doucette R, Peterson EW (2014) Identifying water sources in a karst aquifer using thermal signatures. *Environ Earth Sci* 72:5171–5182. <https://doi.org/10.1007/s12665-014-3387-2>
- Figura S, Livingstone DM, Kipfer R (2015) Forecasting groundwater temperature with linear regression models using historical data. *Groundwater* 53:943–954. <https://doi.org/10.1111/gwat.12289>
- Fleagle RG, Businger JA (1980) An introduction to atmospheric physics, 2nd edn. Academic, London
- Gruszczyński T, Szostakiewicz-Hołownia M (2019) Interpretacja zmienności temperatury wody w źródle na wschodnim stoku Zameczków (Tatry Zachodnie) na podstawie ciągłych obserwacji monitoringowych i numerycznego modelu transportu ciepła [Interpretation of variability of water temperature in a spring

- on the eastern slope of Zameczków (Western Tatras) based on continuous monitoring observations and a numerical model of heat transport]. *Biul Państwowego Inst Geol* 475(475):43–50. <https://doi.org/10.7306/bpig.5>
- Hess M (1965) Pietra klimatyczne w polskich Karpatach Zachodnich [Vertical climatic zones in the Polish Western Carpathians]. *Zesz Nauk Uniw Jagiellońskiego Pr Geogr* 11:1–267
- Humnicki W (2007) Hydrogeologia Pienin [Hydrogeology of the Pieniny Mountains]. Wydawnictwa Uniwersytetu Warszawskiego, Warsaw
- Humnicki W, Szostakiewicz-Hołownia M, Porowski A (2019) Problems in “age” dating of groundwater drained by the Pieniny Springs. *Biul - Państw Inst Geol* 475:59–66. <https://doi.org/10.7306/bpig.7>
- Humnicki W, Szostakiewicz-Hołownia M (2022) Ocena dynamiki drenażu wód podziemnych przez źródła pienińskie z wykorzystaniem głównej krzywej recesji (MRC) [Assessment of groundwater drainage dynamics in the Pieniny springs with application of Master Recession Curves (MRC)]. *Pieniny – Przyr i Człowiek* 18:115–130
- James ER, Manga M, Rose TP, Hudson GB (2000) The use of temperature and the isotopes of O, H, C, and noble gases to determine the pattern and spatial extent of groundwater flow. *J Hydrol* 237:100–112. [https://doi.org/10.1016/S0022-1694\(00\)00303-6](https://doi.org/10.1016/S0022-1694(00)00303-6)
- Kibitlewski S (1987) Cios w bryłach skałkowych serii czorsztyńskiej na spiskim odcinku pienińskiego pasa skałkowego [A joint in klippen bodies of Czorsztyń series on the Spisz section of the Pieniny Klippen Belt]. *Przegląd Geol* 35:497–502
- Kostrakiewicz L (1982) Klimat [Climate]. In: Zarzycki K (ed) *Przyroda Pienin w obliczu zmian* [The nature of the Pieniny in relation to changes]. Zakład Ochrony Przyrody i Zasobów Naturalnych Polskiej Akademii Nauk, Państwowe Wydawnictwo Naukowe, Warsaw-Crakow, pp 53–69
- Kozak J, Zając E (2018) Monitoring temperatury powietrza w rejonie Trzech Koron w latach 1998–2017 [Air temperature monitoring in the area of Trzy Korony over the period 1998–2017]. *Pieniny – Przyr i Człowiek* 15:159–163
- Kurylyk BL, MacQuarrie KTB, Caissie D, McKenzie JM (2015) Shallow groundwater thermal sensitivity to climate change and land cover disturbances: derivation of analytical expressions and implications for stream temperature modeling. *Hydrol Earth Syst Sci* 19:2469–2489. <https://doi.org/10.5194/hess-19-2469-2015>
- Liñán Baena C, Andreo B, Mudry J, Carrasco Cantos F (2009) Groundwater temperature and electrical conductivity as tools to characterize flow patterns in carbonate aquifers: the Sierra de las Nieves karst aquifer, southern Spain. *Hydrogeol J* 17:843–853. <https://doi.org/10.1007/s10040-008-0395-x>
- Long AJ, Gilcrease PC (2009) A one-dimensional heat-transport model for conduit flow in karst aquifers. *J Hydrol* 378:230–239. <https://doi.org/10.1016/j.jhydrol.2009.09.024>
- Luhmann AJ, Covington MD, Peters AJ et al (2011) Classification of thermal patterns at karst springs and cave streams. *Ground Water* 49:324–335. <https://doi.org/10.1111/j.1745-6584.2010.00737.x>
- Manga M (2001) Using springs to study groundwater flow and active geologic processes. *Annu Rev Earth Planet Sci* 29:201–228
- Mohseni O, Stefan HG (1999) Stream temperature/air temperature relationship: a physical interpretation. *J Hydrol* 218:128–141. [https://doi.org/10.1016/S0022-1694\(99\)00034-7](https://doi.org/10.1016/S0022-1694(99)00034-7)
- Munz M, Oswald SE, Schmidt C (2017) Coupled long-term simulation of reach-scale water and heat fluxes across the river–groundwater interface for retrieving hyporheic residence times and temperature dynamics. *Water Resour Res* 53:8900–8924. <https://doi.org/10.1002/2017WR020667>
- Okunev P, Johnson CR (1997) Necessary and sufficient conditions for existence of the LU factorization of an arbitrary matrix. <http://arxiv.org/abs/math/0506382>. Accessed 15 Jun 2023
- Pekárová P, Tall A, Pekár J et al (2022) Groundwater temperature modelling at the water table with a simple heat conduction model. *Hydrology* 9. <https://doi.org/10.3390/hydrology9100185>
- Pletcher RP (2006) Finite-difference method. In: Minkowycz WJ, Sparrow EM, Murthy JY (eds) *Handbook of numerical heat transfer*, 2nd edn. Wiley, Hoboken, NJ, pp 53–90
- Polyakov DG, Arkhangelskaya TA, Ryabukha AG, Kovda IV (2021) Thermal diffusivity of the cryomorph soils of steppe complexes on limestone. *Eurasian Soil Sci* 54:1328–1336. <https://doi.org/10.1134/S1064229321090064>
- Rybach L (2012) Shallow systems: geothermal heat pumps. In: Sayigh A (ed) *Comprehensive renewable energy*. Elsevier, Amsterdam, pp 189–207
- Smerdon JE, Pollack HN, Enz JW, Lewis MJ (2003) Conduction-dominated heat transport of the annual temperature signal in soil. *J Geophys Res Solid Earth* 108:1–6. <https://doi.org/10.1029/2002jb002351>
- Staško S, Buczyński S, Blachowicz M (2021) Temperatura wód podziemnych i jej znaczenie w badaniach hydrogeologicznych [Groundwater temperature and its importance in hydrogeological research]. *Prz Geol* 69:224–233. <https://doi.org/10.7306/2021.12>
- Szczucińska AM, Wasielewski H (2013) Seasonal water temperature variability of springs from porous sediments in Gryżynka Valley, western Poland. *Quaest Geogr* 32:111–117. <https://doi.org/10.2478/quageo-2013-0019>
- Tamburini A, Menichetti M (2019) Groundwater temperature as a natural tracer to characterize hydraulic behaviour and geometry of carbonate aquifers: Mt. Nerone karst system, central Italy. *Rend Online Soc Geol Ital* 47:121–125. <https://doi.org/10.3301/ROL.2019.22>
- Taylor CA, Stefan HG (2009) Shallow groundwater temperature response to climate change and urbanization. *J Hydrol* 375:601–612. <https://doi.org/10.1016/j.jhydrol.2009.07.009>
- Thomson J (2010) Observations of thermal diffusivity and a relation to the porosity of tidal flat sediments. *J Geophys Res Ocean* 115:1–6. <https://doi.org/10.1029/2009JC005968>
- van Wijk WR (1965) Soil microclimate, its creation, observation and modification. In: Waggoner PE, Gates DM, Webb EK et al (eds) *Agricultural meteorology*. American Meteorological Society, Boston, pp 59–73
- W-shi Wang, Oswald SE, Gräff T et al (2020) Correction: Impact of river reconstruction on groundwater flow during bank filtration assessed by transient three-dimensional modelling of flow and heat transport (*Hydrogeology Journal*, (2020), 28, 2, (723–743), DOI: 10.1007/s10040-019-02063-3). *Hydrogeol J* 28:2633–2634. <https://doi.org/10.1007/s10040-020-02221-y>
- Wierzbowski A, Aubrecht R, Krobicki M et al (2004) Stratigraphy and palaeogeography position of the Jurassic Czertezik Succession, Pieniny Klippen Belt (Western Carpathians) of Poland and eastern Slovakia. *Ann Soc Geol Pol* 74:237–256
- Williams GP, Gold LW (1976) Ground temperatures. *Can Build Dig* CBD-180: <https://doi.org/10.4224/40000712>
- Wojkowski J, Skowera B (2017) Relation of soil temperature with air temperature at the Jurassic River Valley. *Inżynieria Ekol* 18:18–26. <https://doi.org/10.12912/23920629/65855>
- World Meteorological Organization (2018) *Guide to instruments and methods of observation (WMO-No. 8) volume I: measurement of meteorological variables*, 2018th edn. WMO, Geneva
- Zaszewski D, Gruszczyński T (2022) A low-cost automatic system for long-term observations of soil temperature. *Geomatics Environ Eng* 17:75–101. <https://doi.org/10.7494/geom.2023.17.1.75>
- Zhang T (2005) Influence of the seasonal snow cover on the ground thermal regime: an overview. *Rev Geophys* 43. <https://doi.org/10.1029/2004RG000157>